Ion Thruster Produced Roll Torque

Neil A. Arthur*
Vantage Partners LLC, Cleveland, OH, 44142, USA

Disturbances to the ion engine's thrust vector will cause a spacecraft to spin about its axis if left unmanaged. Spin about the yaw and pitch axis can be easily handled by a gimbal with enough authority. Spin about the roll axis however must be handled by additional thrusters or reaction wheels. In order to capitalize on the high efficiency of their thrusters, missions utilizing electric propulsion as primary propulsion generally include long periods of thrusting (several years). It is necessary to quantify and understand the ion thruster produced roll torque because it will define the amount of chemical propellant that must be carried or the lifetime and quantity of momentum wheels required for the mission. The roll torque produced by the NEXT ion thruster is analyzed through a combination of theoretical calculations and magnetic field simulations. Experimental techniques for measuring roll torque and past flight data are also discussed.

I. Nomenclature

$\vec{B}$	=	Magnetic field
$\vec{E}$	=	Electric field
$\vec{F}$	=	Lorenz force
f	=	Focal length
F_s	=	Screen grid open area fraction
j_b	=	Beam current density
j_CL	=	Child-Langmuir limited current density
ℓ_a	=	Acceleration length
ℓ_g	=	Deceleration length
l_g	=	Grid gap
M_i	=	Ion mass
q	=	Elementary charge
$\dot{Q}_\mathrm{m}$	=	Mass flux
r_0	=	Grid radius of curvature
T_A	=	Aperture misalignment produced torque
T_B	=	Magnetic field produced torque
V_b	=	Beam voltage
V_N	=	Net voltage
V_T	=	Total voltage
α	=	Doubly-charged ion ratio
β	=	Beamlet deflection angle
δ	=	Aperture misalignment distance
κ	=	Misalignment angle constant of proportionality
τ_B	=	Magnetic torque density

II. Introduction

Ion thrusters utilize a pair of grids to electrostatically accelerate ions to high velocity and produce thrust. Each electrode has anywhere from hundreds up to a hundred thousand small holes through which the ions exit the thruster. These holes which are on the order of 1 mm^2 must be aligned to the corresponding hole on the paired grid, over the

*Aerospace Engineer, Electric Propulsion Systems Branch, AIAA Member.

full thruster diameter of ~0.5 m. When the corresponding apertures of the screen and accelerator grid are not aligned, the ions passing through the paired holes will be deflected. Misalignment errors on the order of 10 µm between the centerline of paired holes can produced large disturbances to the thrust vector when summed over the full area of the grid. Additionally, the magnetic field, which is used to confine charged particles in the discharge chamber, can interact with ions in the thruster beam. In the presence of magnetic fields, charged particles will undergo Larmor motion and spiral about the magnetic field lines. This motion creates an off-axis thrust component. The goal of this paper is to discuss and quantify the sources of roll torque that arise from both grid misalignment errors and beam ion–magnetic field interactions. A third theorized source of roll torque is the placement of the neutralizer cathode, however this has been dismissed because the magnitude of such roll torque based on the electric field created between the neutralizer and beam would be orders of magnitude less than the values observed in flight [1–3].

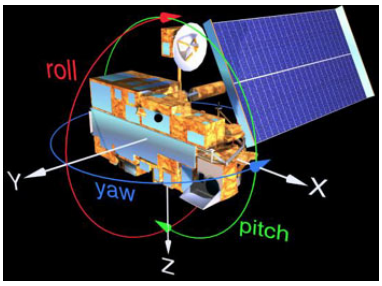

Fig. 1 Yaw, pitch, and roll axis of a spacecraft traveling in the $\vec{x}$-direction [4].

A grid misalignment error that is normal to the thrust axis (translation error) will produce torques about the spacecraft yaw and pitch axis. The spacecraft's yaw, pitch, and roll axis are shown in fig. 1 and an example of a grid translation error is shown in fig. 2. For ion thrusters, these off-axis rotations are typically mitigated by the ion thruster gimbal, which generally has a range of at least a few degrees. If the apertures are misaligned such that the accelerator grid is 'clocked' relative to the screen grid, a torque is produced about the roll axis, shown in fig. 3. This so-called roll torque is not easily managed by the gimbal and requires reaction wheels or additional thrusters to balance the torque. This

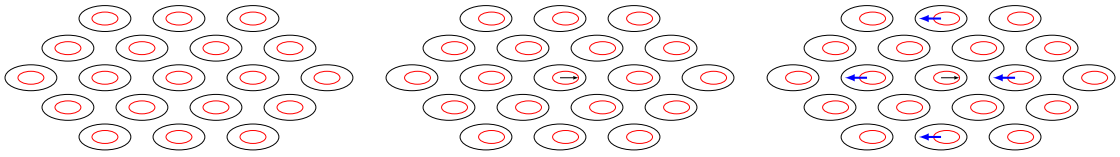

(a) Apertures of an aligned grid. **(b) Accelerator apertures translated to the right.** **(c) Beamlets deflected to the left.**

Fig. 2 Depiction of a grid translation that produces a spin about the yaw or pitch axis. Screen grid and acclerator grid apertures are shown in black and red, respectively. The ion beamlet deflections are shown with blue arrows. Not to scale.

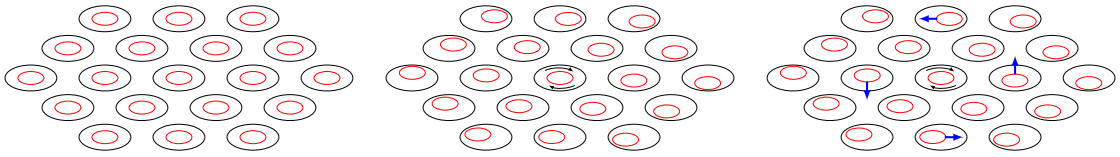

(a) Apertures of an aligned grid. **(b) Accelerature apertures misaligned 2° clockwise.** **(c) Beamlets deflected counterclockwise.**

Fig. 3 Depiction of a grid clocking error that produces a roll torque. Screen grid and acclerator grid apertures are shown in black and red, respectively. The ion beamlet deflections are shown with blue arrows. Not to scale.

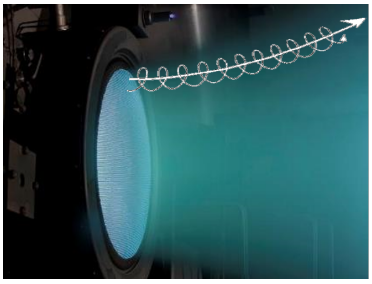

Fig. 4 Illustration depciting ions orbiting magnetic field lines that leak from the discharge chamber into the beam.

torque must be quantified because during a mission it drives the amount of secondary propellant that must be carried or the number and type of momentum wheels required. Electric propulsion devices, and ion thrusters in particular, have extremely long lifetimes and sufficient roll torque mitigating devices must be carried to last the life of the mission [5]. Previous studies have examined ion optics misalignment and its effect on beamlet deflection, without specifically addressing roll torque [6–13]. These studies are expanded upon and adapted specifically to grid clocking errors and roll torque.

Another mechanism for producing roll torque is magnetic field interactions with beam ions. In the case of an ion thruster, the velocity of the ions is approximately normal to the surface of the grid and magnetic field is in general azimuthally symmetric. It then follows that the Lorenz force will be perpendicular to the velocity vectors, in the azimuthal direction such that a torque is produced. The magnetic field vectors can be obtained through the use of commerically available electromagnetic modeling software and compared to measurements. While the grid misalignment error torque is produced at the grid surface as ion beamlets are deflected, the magnetic field torque is produced throughout the entire volume of the beam.

Roll torque data collected in-space for ion thrusters is limited. NASA's Deep Space 1 experienced a roll torque of 10 µN m in space while operating with a single NSTAR thruster and used hydrazine thrusters to mitigate roll motion [3, 14, 15]. During the mission, measures were taken to conserve hydrazine as it was critical to maintain proper solar array and spacecraft pointing; once the spacecraft could no longer manage proper pointing the mission was terminated [16, 17]. NASA's Dawn mission had three NSTAR thrusters that produced roll torques from 25 to 55 µN m [3]. The Dawn mission used reaction wheels for roll control and hydrazine thrusters for reaction wheel unloading. The Dawn mission ended in November 2018 when the spacecraft ran out of hydrazine and was no longer able to control pointing of the spacecraft [18]. Both NASA missions that have used ion thrusters demonstrate the importance of properly quantifying the roll torque prior to launch, as the lack of sufficient hydrazine propellant used for roll control ultimately caused the missions to be terminated (well after they had completed their primary objective and extended missions). Pre-flight thruster manufacture data (grid clocking misalignments, magnetic field measurements) is more limited than published in-space roll torque values, but comparisons will be made with pre-flight roll torque estimates to the extent possible. The upcoming DART mission and a proposed New Frontiers mission utilizing the NEXT-C thruster have also requested refined roll torque calculations due to the importance such calculations have on their hydrazine budget.

III. Misalignment Produced Roll Torque

A. Beamlet Deflection due to Grid Misalignment

To determine the magnitude of misalignment produced roll torque, the degree to which the ion beamlets are deflected by the aperature misalignment must be estimated. Whealton considered the grids to be simple pair of lenses and used linear optics theory to determine the amount of deflection produced by a given amount of misalignment [6]. Whealton's approach is shown schematically in fig. 5, and using this, the ion optics can be approximated as a thin lens with a focal length given by

$$f = \frac{4V_T}{E_1 - E_2} \tag{1}$$

where where V_T is the total accelerating voltage, E_1 is the electric field upstream of the accelerator grid, and E_2 is the electric field downstream of the accelerator grid [7]. The accelerating field, E_1 is the total voltage, V_T, over the

acceleration length, ℓ_a.

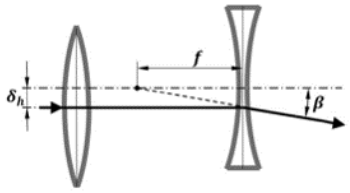

Fig. 5 An optical approximation of the two grid geometry showing the angle, β produced by a misalignment error, δ [13].

The total accelerating voltage is the difference between the screen voltage V_S and the accelerator voltage V_A, $V_T = V_S - V_A$. The net accelerating voltage is $V_N = V_S + V_A$, where V_A is always negative for ion beams. Figure 5 shows the deflection of light produced by a misalignment of two lenses. Using the same theory for the ion optics, the beamlet deflection angle, β, is proportional to the grid deflection over the focal length

$$\beta = \frac{\delta}{f} \tag{2}$$

where δ is the amount of misalignment between the screen and accelerator aperture. Substituting in the focal length from equation (1) gives

$$\beta = \frac{\delta(E_1 - E_2)}{4V_T} \tag{3}$$

In the limit that $|E_2| \ll |E_1|$, $\ell_a \approx l_g$, and $E_1 \approx V_T/l_g$, β can be rewritten

$$\beta = \frac{\delta}{4l_g} \tag{4}$$

which is

$$\beta = 14.3^\circ \frac{\delta}{l_g} \tag{5}$$

where β is in degrees. Let κ be the constant of proportionality, $\kappa = 14.3^\circ$ in equation (5). This is the theoretical value derived by Whealton [6, 8, 10]. Stewart included the effects of space charge in a simple parallel plate geometry, where the electric field becomes $E_1 \approx 4V_T/3l_g$, and the expression for β becomes

$$\beta = 19.1^\circ \frac{\delta}{l_g} \tag{6}$$

where κ increases to 19.1° [8].

A variety of studies were untaken to determine the validity of linear optics theory and specifically the value of κ that is appropriate. Homa and Wilbur found experimentally that $\kappa = 15.8^\circ$ [10]. Haag found that for NSTAR optics κ ranged from 16.5° to 22.8° as the power level was increased from 0.98 kW to 2.3 kW [11]. Okawa used a 3D PIC simulation to estimate that κ could be as high as 20.0° [12]. Shagayda used a 3D ion optics code to model beamlet deflection and found that the value of κ was close to the space charge limit of 19.1° [8, 13].

These studies have found a 10–60% increase in the value of κ over the theoretical value. One reason, suggested by Homa, is that the assumption $|E_2| \ll |E_1|$ is not a good approximation [7]. As the ratio $|E_2|/|E_1|$ increases, the value of β increases. For a given grid geometry and throttle level, the values of $|E_2|$ and $|E_1|$ can be estimated. The deceleration electric field, E_2 is

$$E_2 = \frac{V_T - V_N}{\ell_d} \tag{7}$$

where l_d is the deceleration length. For a two grid geometry, the deceleration length is not easily defined and must be estimated from an expression provided by Kaufman [19]. The deceleration length is the distance between the accelerator grid and the ion beam neutralization plane, which is depicted in fig. 6 [5, 7]. The deceleration length can be written

$$\ell_d = \ell_a \sqrt{\frac{1 + 3\sqrt{R} - 4R\sqrt{R}}{F_s} \frac{j_b}{j_{CL}}} \tag{8}$$

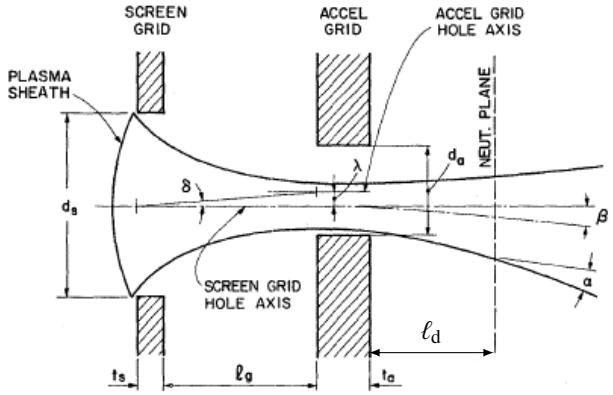

Fig. 6 Two grid system showing the neutralization plane and corresponding deceleration length [5].

where F_s is the open area fraction of the screen grid, j_b is the beam current density, j_{CL} is the Child-Langmuir limited current density, and R is the ratio

$$R = \frac{V_N}{V_T} \tag{9}$$

Homa and Wilbur estimate that the correction $(1 - E_2/E_1)$ for the grids they analyzed was 1.14, or a 14% increase in β, and their experimentally determined β was 10% higher than the theoretical value in equation (5). For the NSTAR grids in Haag's study $(1 - E_2/E_1)$ ranges from 1.06 to 1.23. The experimentally determined values were as much as 60% higher. This likely resulted from using the cold grid gap, which has been found to decrease by as much as 55% during full power operation [20, 21]. For the grid geometry used by Okawa, $(1 - E_2/E_1)$ ranges from 1.19 to 1.40. The value of κ reported by Okawa was also 40% higher than the theoretical value. For the NEXT grid geometry, $(1 - E_2/E_1)$ ranges from 1.07 to 1.19. These correction factors can be applied to equation (5).

B. Beamlet Deflection Produced Roll Torque

The roll torque produced by misaligned ion optics apertures can be written

$$T_A = \int_A \vec{\ell} \times \dot{Q}_m \vec{v}_\phi \, dA \tag{10}$$

where $\vec{\ell}$ is the moment arm with respect to the axis passing through the spacecraft center of mass, $\dot{Q}_m$ is the mass flux of xenon ions, and $\vec{v}_\phi$ is the ion velocity in the azimuthal direciton [22]. The roll torque is integrated over the area of the grids. Equation (10) can be rewritten in grid-oriented spherical coordinates:

$$T_A = r_0^2 \int_0^{2\pi} \int_0^{\theta_{max}} \dot{Q}_m \vec{v}_\phi \sin\theta \, d\theta \, d\phi \tag{11}$$

where r_0 is the grid radius of curvature. The moment arm $\vec{\ell}$ is equal to $r_0 \sin\theta$, and the mass flux, $\dot{Q}_m$ is equal to $M_i j_b / q$, where $j_b(r, \phi, \theta)$ is the beam current density. The beam current density can be inferred from a combination of experimental measurements, simulations, and some assumptions. The azimuthal ion velocity, $\vec{v_\phi}$, is approximated as the typical ion velocity deflected by the grid aperture misalignment:

$$v_\phi = \sqrt{\frac{2qV_b}{M_i}} \sin\beta(\theta) \tag{12}$$

where β is the beamlet deflection angle taken from equation 5, and the sin is taken to give the velocity component normal to the beam direction. Equation 10 then becomes

$$T_A = 2\pi r_0^3 \sqrt{\frac{2V_b M_i}{q}} \alpha \int_0^{\theta_{max}} j_b(\theta) \sin[\beta(\theta)] \sin^2\theta \, d\theta \tag{13}$$

The factor α is the thrust loss due to doubly charged ions. This is added to the equation to account for the fact that the measured beam current density over-predicts the number of ions that actually exit the thruster to form the beam. The value of α typically ranges from 0.977 to 0.990. In the case of a grid clocking error, the deflection angle, β varies across the grid face. If the misalignment distance at the edge aperature is equal to $\delta_{\max}$, then the misalignment across the grid can be expressed as

$$\delta(\theta) = \frac{\sin\theta}{\sin\theta_{\max}}\delta_{\max} \tag{14}$$

Substituting into equation (13) gives

$$T_{\mathrm{A}} = 2\pi r_0^3 \sqrt{\frac{2V_{\mathrm{b}}M_{\mathrm{i}}}{q}}\alpha \int_0^{\theta_{\max}} j_{\mathrm{b}}(\theta) \sin\left[\kappa \frac{\sin\theta}{\sin\theta_{\max}} \frac{\delta_{\max}}{\ell_{\mathrm{g}}}\right] \sin^2\theta \, d\theta \tag{15}$$

where the value of κ must be chosen appropriately and the integral is done numerically from the approximated current density at the grid exit plane.

(a) Ion velocity vectors normal to grid shown along a single radius along the grid surface.

(b) Magnetic field vectors at the grid surface shown along a single radius.

Fig. 7 Ion velocity and magnetic field vectors showing the components of the Lorenz force which produce roll torque.

IV. Magnetic Field Produced Torque

The ions produced by the thruster are subject to the Lorenz force

$$\vec{F} = q\left(\vec{E} + \vec{v} \times \vec{B}\right) \tag{16}$$

where the ion optics use an electric field to accelerate the ions and provide thrust in the direction of motion, but the magnetic circuit within the thruster also causes ions to orbit about the $\vec{B}$-field lines, producing a force that is perpendicular to the direction of ion motion. The velocity of the ions is approximately normal to the grid surface, or in the $\hat{r}$-direction, shown in fig. 7a. The magnetic field at the thruster's ion optics has a negligible $\hat{\phi}$-component, and is mostly directed in the $\hat{r}$- and $\hat{\theta}$-directions. This creates a roll torque, and is in general the case for ring-cusp ion thrusters because the magnetic field is produced by rings of magnets which are azimuthally symmetric. The magnetic field along a single radius at the accelerator grid is shown in fig. 7b. The magnetic field vectors are obtained through the use of a commercial electromagnetic solver program, which has been validated against measured magnetic field data. The calculation of the Lorenz force is illustrated in fig. 8. The Lorenz force increases exponentially towards the edge of the grid because the magnetic rings are at the outer diameter of the discharge chamber and the magnetic field is strongest there.

The Lorenz force density is found by multiplying the force by the ion density, and the current density is equal to $\vec{j} = qn\vec{v}$. Therefore, the magnetic field torque density is

$$\tau_{\mathrm{B}} = \vec{\ell} \times \left(\vec{j} \times \vec{B}\right) \tag{17}$$

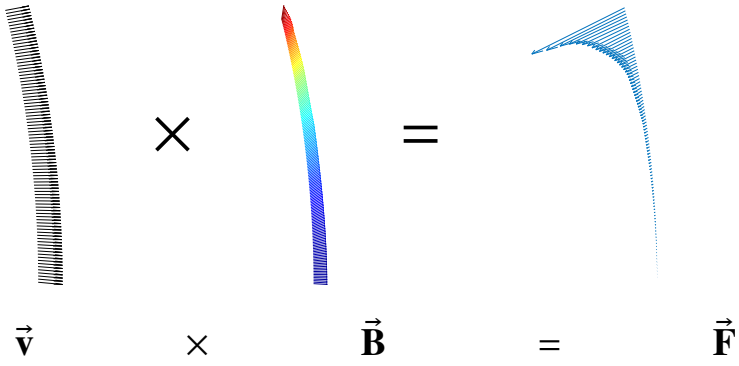

Fig. 8 Calculation of the Lorenz force.

The total torque produced by the ions in the plume is found by integrating this equation

$$T_{\mathrm{B}} = \int_0^{2\pi} \int_0^{\theta_{\max}} \int_{r_{\mathrm{grid}}}^{\infty} \vec{\ell} \times \left(\vec{j}(r,\theta) \times \vec{B}(r,\theta) \right) r^2 \sin\theta \, dr \, d\theta \, d\phi \tag{18}$$

Simplifying equation 18 slightly by assuming that the measured beam current dennsity, $|j|$, is directed in the $\hat{r}$-direction only (normal to grid), such that only the B_θ and B_ϕ components contribute to roll torque, and $B_\phi \approx 0$,

$$T_{\mathrm{B}} = 2\pi \int_0^{\theta_{\max}} \int_{r_{\mathrm{grid}}}^{\infty} j_r(r,\theta) \, B_\theta \sin^2\theta \, r^3 dr \, d\theta \tag{19}$$

The value of $\theta_{\max}$ is the value of θ at which the beam current falls to zero. This value is larger than the angle subtended by the grid because as the beam travels downstream it diverges or expands to larger angles. Similarly, while the magnetic field and ion plume theoretically extend to $r \to \infty$, the magnitudes fall off according to r^{-3} and measurement data is only available up to a finite distance from the thruster.

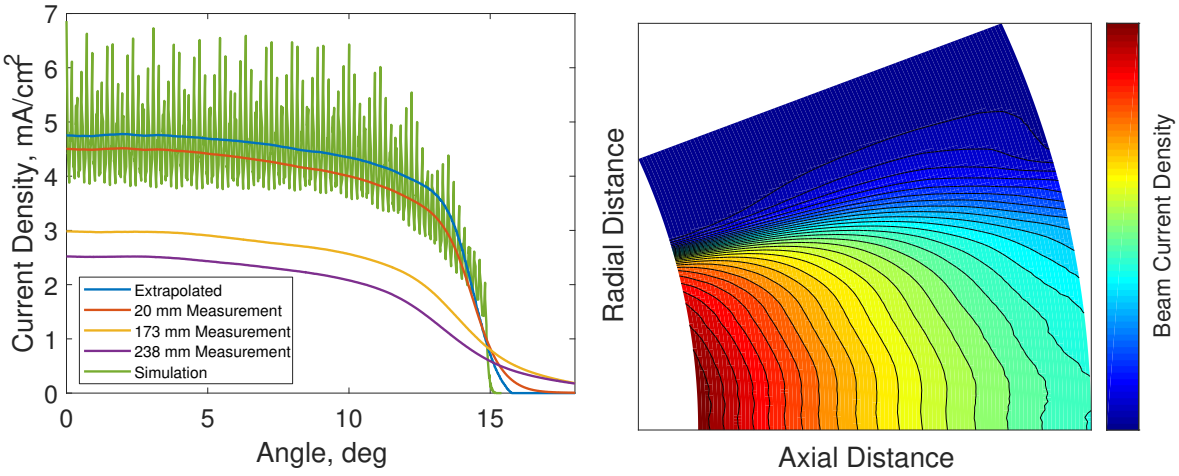

(a) Measured and simulated beam current.

(b) Beam current density throughout the plume.

Fig. 9 NEXT beam current density interpolated from measurements.

V. Calculations

Figure 9a shows NEXT full power beam current measurements at three different distances from the accelerator grid as well as the simulated beam current, which has a peaked profile due to the simulation resolving individual apertures.

From the experimental measurements, an average profile across the grid face is calculated by extrapolating from 20 mm back to the grid. Repeating this extrapolation/interpolation procedure at various distances from the grid leads to fig. 9b which is a two-dimensional plot of beam current density through the plume. The extrapolated profile in fig. 9a is used to calculate the roll torque due to grid clocking errors, and the two-dimensional plot in fig. 9b is used for integrating the magnetic field produced roll torque throughout the plume.

Using the extrapolated beam profile and the equation for β, the roll torque produced by a NEXT-C ion thruster as a function of grid misalignment is shown in fig. 10a. The grid clocking error is the distance between screen and accelerator centers at the outermost hole pairs. This is generally how the alignment of the grids for flight programs is specified, e.g. misalignment shall be ≤X.Xmm at the beam periphery. The solid line assumes $\kappa = 15.8°$, which is the value determined by Homa and Wilbur, through the only experimental study of beamlet deflection as a function of grid misalignment. This value of κ seems to be used as the standard in literature [7, 11, 22, 23]. The roll torque for the maximum specified of misalignment is about 350 µN m. The shaded area in the figure applies the electric field correction, $1 - E_1/E_2$, to the theoretical value of β in equation (5). This electric field correction is a function of thruster power, or throttle condition, and the highest power is 1.19. The maximum, or worst case, roll torque then is 381 µN m. The values in fig. 10a can be roughly scaled to any power level by multiplying the curve by ratios of $j_b\sqrt{V_b}$ at the desired throttle level, to the full power level. The NEXT thruster has a flat enough beam profile at all throttle conditions, a grid gap that is roughly constant with power, such that this scaling provides a good estimate without re-integrating equation (15) [24].

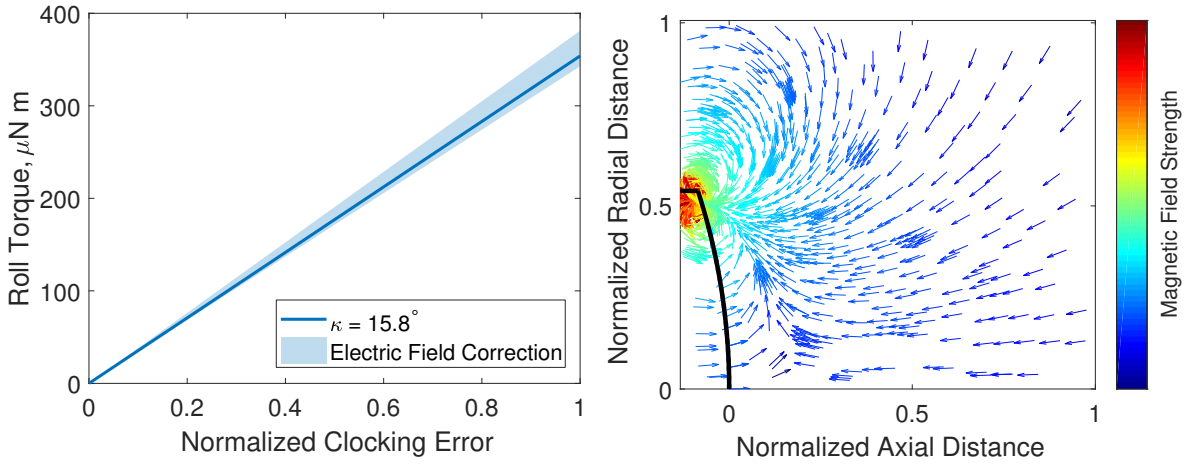

(a) Grid clocking produced roll torque as a function of misalignment at the outermost apertures.

(b) Magnetic field vectors used to calculate roll torque. An outline of the NEXT-C thruster is shown for orientation.

Fig. 10 The grid clocking produced roll torque and the magnetic field vectors which produce roll torque.

The magnetic field roll torque is calculated by crossing the current density in fig. 9b and the magnetic field vectors in fig. 10b, and then numerically integrating over the beam volume up to a chosen distance from the grid plane. Ideally, beam current density measurements exist up to several thruster diameters away from the thruster, that can be corrected for facility charge exchange effects. From this calculation, the NEXT-C ion thruster magnetically induced roll torque at full power is estimated to be ~32 µN m. This calculation agrees well with NSTAR magnetic roll torque estimates when you account for the fact that NEXT is larger, operates at higher beam currents and voltages, and has a much flatter beam profile than NSTAR. All these factors suggest that the magnetic field roll torque experienced by NEXT should be ~ 4.5× NSTAR.

VI. Measurements

Prior studies have utilized laser induced fluorescence to measure the azimuthal velocities on xenon ions in the plume to estimate roll torque [25–27]. This study used a probe to measure the ion flow velocity direction. A modified Mach probe is swept across the face of the thruster, and the current measured from each face of the Mach probe is compared to ascertain the ion flow direction [28–31]. A schematic of the probe in front of an ion thruster is shown in fig. 11 along

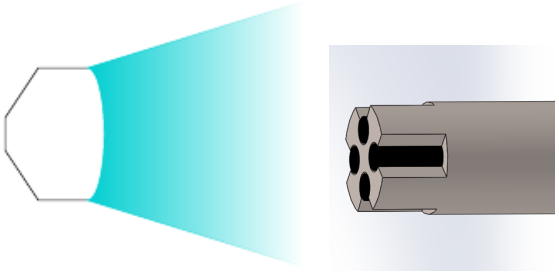

(a) Schematic of a roll torque probe in front of an ion thruster.

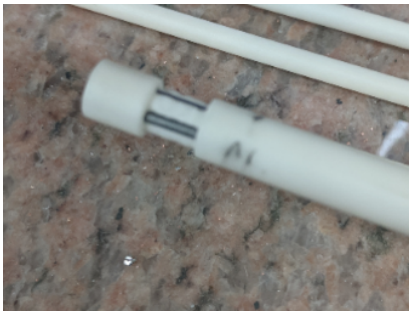

(b) Photograph of roll torque probe.

Fig. 11 Schematic and photograph of a roll torque probe.

with a photograph of the actual probe used. The probe schematic is sectioned to allow a view of the ion collectors.

The probe is scanned from left to right across the face of the thruster, and for the purposes of measuring roll torque, the ion current collected by the top and bottom probes are compared. Figure 12 shows the measured Mach number. The solid, horizontal, black line represents '0' flow, or equal current to both probes. The dashed line represents the expected measurement shape assuming that the grid set only has rotational misalignment. However, the data suggests that there is a translational misalignment which directs the beam in the downward direction. This fact agrees qualitatively with unpublished thrust vector data taken with this thruster in two separate facilities [32, 33]. Detailed grid misalignment measurements are not available for this thruster because it is an engineering model NEXT thruster and not part of a flight program.

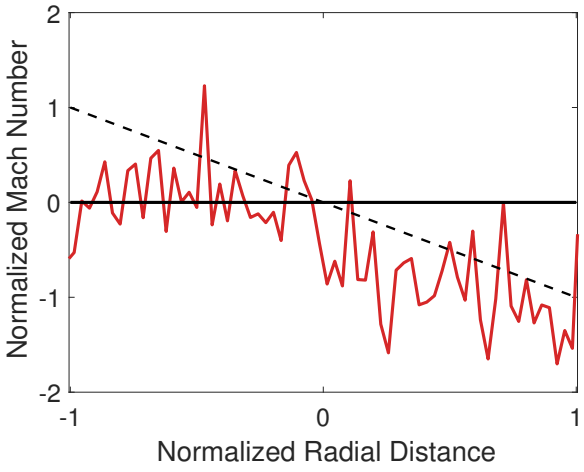

Fig. 12 Data taken with the roll torque probe showing the ratio of the current collected by the top and bottom probe. The solid black line denotes 0. The dashed black line approximates what would be expected for a grid pair that only has rotation errors and no translation error.

VII. Dawn Flight Thrusters

NASA's Dawn mission utilized three NSTAR ion thrusters to travel to Vesta and Ceres in the asteroid belt [34]. The Dawn mission measured each thruster's roll torque using the momentum buildup in the reaction wheels [3, 35]. In this section, the methodology used for calculating roll torque for the NEXT thruster is validated against Dawn flight data.

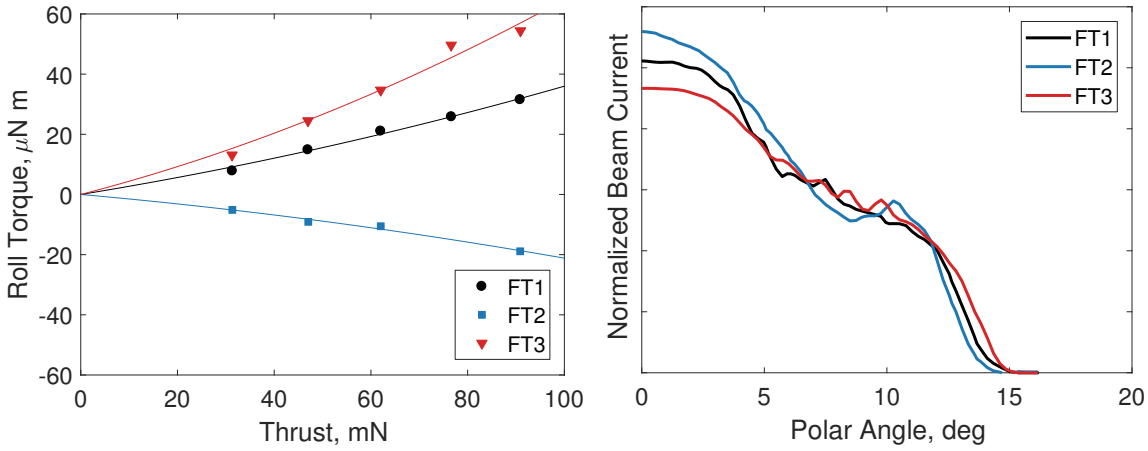

(a) Dawn flight thruster roll torque measured in space [3]. **(b) Dawn flight thrusters beam current profiles measured on the ground pre-launch.**

Fig. 13 Beam current and roll torque data from the Dawn flight thrusters.

Figure 13a shows the measured roll torque as a function of thrust, showing that flight thruster 2 produced the lowest amount of roll torque in a direction opposite the other two thrusters. Figure 13b shows the measured beam profiles of each flight thruster prior to launch, showing that flight thruster 2 has the most peaked beam profile. This is consistent with producing the lowest roll torque, as it is the thruster with the least current near the periphery of the grids, where most of the torque is produced. The relative misalignment between the screen and accelerator grid on each grid set was measured pre-flight at ~25 apertures along 3 radii to determine the effective clocking misalignment and predict the roll torque [36]. The misalignments are not a simple rotation so the calculation is not straightfoward. There is also a translation component, and the true position of the holes has an associated tolerance. From these measurements, an effective translation and rotation matrix can be calculated using a least-squares algorithm, or an effective rotation can be determined through curve fitting the measured hole positions. The misalignment measurements were used to calculate the roll torque for flight thrusters 1, 2, and 3, which was predicted at full power to be about 16, –15, and 23 μN m respectively. From fig. 13a, it can be seen that the in-flight measured values were about 32, –25, and 54 μN m, corresponding to a pre-flight underprediction of between 40 and 60%.

An interesting phenomena observed on Dawn is that the roll torque for flight thruster 3 decreased the longer the thruster was operated. Figure 14a shows the measured roll torque as a function of xenon propellant throughput [37]. One possible explanation provided by Garner is that there is a systematic thrust vector error that results in a torque, which is changing as xenon is used and the spacecraft's center of mass changes [37]. Another explanation is that the grid misalignment has improved during operation, possibly as badly misaligned apertures are severely eroded. The relatively rapid erosion of badly misaligned edge apertures is a documented process that has been referred to as 'notching' [39, 40]. However, the measured accelerator current for flight thruster 3 in fig. 14b shows a <10% increase in current, which does not suggest significant grid erosion.

Flight data for ion thrusters is limited so it is worth understanding why the predicted values are off by a factor of 2 for the Dawn mission. First, it is crucial to understand the gap between the screen and accelerator grid. From equation (5), the beamlet deflection angle is inversely proportional to the grid gap, and the roll torque is proportional to $\sin\beta$. The pre-flight predictions utilized a grid gap that was determined from a study by Haag that used a translatable accelerator grid to steer the ion beam [11]. The amount of steering in the beam per accelerator grid translation was fit to Homa and Wilbur's equation for β to determine that the grid gap was 0.48 mm. This gap also agreed with a finite element thermal model of the thruster, which neglects electrostatic deflection effects. Once a dedicated study was undertaken to measure the grid gap on centerline of the NSTAR thruster during operation, it was determined that the grid gap was actually -0.360 ± 0.075 mm, where the negative sign indicates the value is relative to the cold grid gap [20]. This leads to a

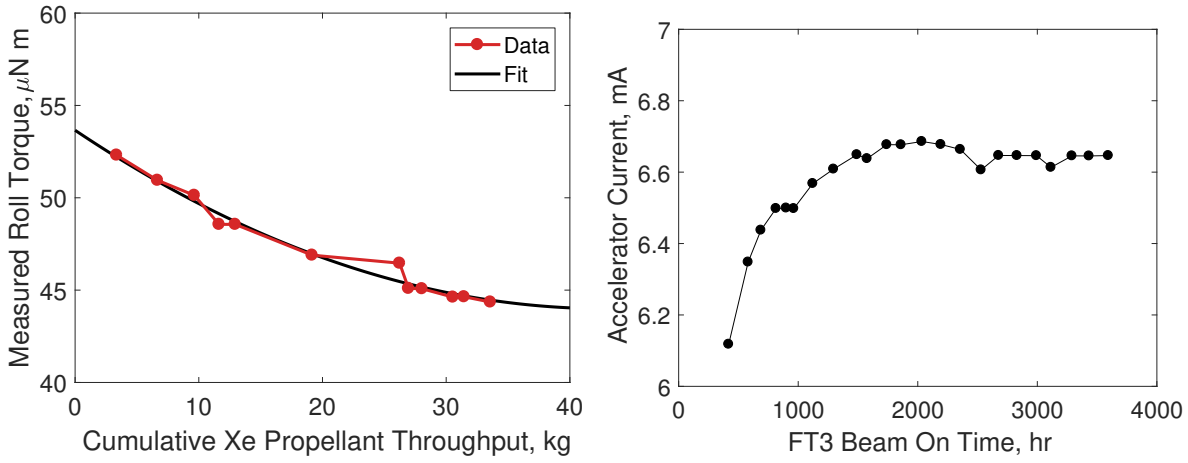

(a) Flight thruster 3 roll torque as a function of xenon propellant throughput [35, 37].

(b) Flight thruster 3 accelerator current as a function of thruster operation time [37, 38].

Fig. 14 Roll torque and accelerator current measured on Dawn's flight thruster 3 as a function of operational time and propellant throughput.

significant increase in the calculated roll torque.

Additionally, the grid gap is generally assumed to be constant across the grid face. However, optical and gapping gauge measurements of various thrusters show that the grid gap actually has a 'W' shape, where the gap is largest in the middle and at the edges near the mounting rings, and decreases along a radius. Coincidentally, the edges of the grid are also where most of the roll torque is produced. Accounting for this can lead to an increase in roll torque of ~25% to 30%. Grid gap measurements were made for all three flight thrusters, and they were found to exhibit this W profile.

As shown in fig. 13b, each thruster has its own beam shape profile. This can be due to source effects within the discharge plasma, subtle differences in the magnetic field, or due to variations in the optics themselves. The differing beam profiles in the figure have a noticeable effect on calculated roll torque; >15% between flight thruster 2 which has the most peaked profile and flight thruster 3 which has the most current near the edge of the beam. To get the most accurate estimate of roll torque both the measured beam current density and the measured grid gap for an individual thruster should be used.

Taking into account simply the measured grid gap of –0.36 mm, known grid gap variation, and measured beam profiles, the roll torque estimated for Dawn can be improved to 26, –22, and 38 μN m for flight thrusters 1, 2, and 3 respectively. If you assume the worst case grid gap of –0.435 mm, the predicted roll torque values jump to 35, –29, and 51 μN m. This actually over predicts the roll torque for thrusters 1 and 2, but still slightly under predicts for thruster 3. At this point, the magnetic field induced roll torque can be considered, which has been estimated to be 2 to 7 μN m, and can be either parallel or anti-parallel to the misalignment torque. Suggesting that the worst-case roll torque for flight thruster 3 increases to 58 μN m.

Up to this point, the Dawn roll torque calculations have assumed Homa and Wilbur's experimentally determined value of $\kappa = 15.8°$. Taking into account, the electric field correction suggested by Homa, κ increases by 23% over the theoretical value for NSTAR's full power operating condition, leading to $\kappa = 17.6°$. For a grid gap of –0.36 mm, the roll torque values are calculated as 29, –24, and 43 ± 7 μN m for the three thrusters.

At this point, the predicted roll torque very closely matches the values observed in flight. It should also be noted that flight thruster 2 had a magnetic field configuration that was reversed relative to the other two thrusters. From the calculations, this suggests that the magnetic field induced roll torque was actually in the same direction as the grid misalignment produced roll torque for each thruster (i.e. thruster 1 lies between 31 to 36 μN m and thruster 2 lies between −26 to −31 μN m).

Given that there is uncertainty in the hot grid gap measurement of ±25%, measured on a sample size of a single thruster, it is likely that the actual flight thrusters do no operate with a –0.36 mm grid gap at the center aperture. It is possible that thruster 3 had a slightly smaller grid gap and thruster 2 had a slightly larger grid gap. Also, it is assumed that the grid gap 'W' profile, which is measured cold, maintains the same shape as the grids heat up during thruster firing.

There have not been any studies measuring the hot grid gap profile along a radius. The aperature alignment data is taken at approximately 25 holes (out of thousands) along only 3 radii. In order to improve predictions, measuring aperature alignments at more radii is required. Multiple options exist for addressing the effects of the expected roll torque for missions that utilize ion thrusters. One option is to just carefully consider the absolute worst case, and budget hydrazine accordingly. This would have led to a predictions for Dawn of 47, -40, and 64 μN m, which would have encompassed the observed values. The other option, if carrying extra hydrazine is not possible, is to clearly understand the hot grid gap magnitude and shape as well as measure enough aperture misalignments to more precisely estimate clocking errors.

Finally, the direction of roll torque in fig. 13a should be addressed. This figure has been published in several papers, which state,

> "The direction of the roll torque produced by FT2 corresponds to the right-hand rule with your thumb pointing in the direction of the ion beam propagation [3]."

This means that a negative roll torque follows the right-hand rule with respect to the ion beam vector. The paper goes on to say,

> "However, calculations of the roll toque for each thruster based on careful measurements of the grid clocking errors made during thruster assembly do not agree with the data [in fig. 13a]. These calculations do not correctly predict the magnitudes or even in some cases the directions of the measured roll torque [3]."

The paper claims that the directions of the roll torque are consistent with the directions that would be expected from the magnetic field, however the magnetic field produced roll torque is calculated to be an order of magnitude less than the observed roll torque (consistent with ≤ 7 μN m). The original grid clocking error measurements and the roll torque calculation documents have been re-examined, and in the documents the following statement appears:

> "A positive value for the above roll torque indicates that the beamlets are deflected in the clockwise direction as determined when facing upstream toward the accelerator grid. The torque on the spacecraft, then, is in the 'positive' direction according to the right-hand-rule with your thumb pointing in the direction of the ion beam propagation [36]."

This statement is in opposition to the statement reported in literature. It seems that the detailed calculations made by the Dawn team, based on optics misalignment, *actually did predict the correct direction*, and in fact the magnetic field produced roll torque was in the same direction. This means that measuring grid aperture alignments is a valid method for predicting both the direction and magnitude of the roll torque for future missions.

VIII. Conclusion

Ion thrusters produce a roll torque about the thrust axis due to both rotational grid misalignments and the magnetic field which leaks out into the plume. This effect is non-neglible and must be considered for future ion thruster flights. Both of NASA's deep space missions utilizing ion thrusters utilized hydrazine to counteract the ion thruster produced roll torque, and both missions were ended when the on-board hydrazine was depleted. At least in the case of Dawn, the roll torque estimated prior to launch was less than the actual roll torque observed in flight. However, the clocking misalignment measurements correctly predicted the directions of roll torque. This paper presents updated calculations, with suggested methods for improving roll torque estimates. A method of measuring roll torque using an electrostatic probe also agreed qualitatively with thrust vector measurements made on the same thruster.

Acknowledgments

The NEXT-C project is supported by the Planetary Science Division of the Science Mission Directorate, NASA Headquarters. The assisstance of Chuck Garner at NASA JPL, who provided the Dawn pre-flight grid alignment measurements and roll torque calculations, is greatly appreciated.

References

[1] Patterson, M. J., and Mohajeri, K., "Neutralizer Optimization," *22nd International Electric Propulsion Conference*, Viaregio, Italy, 1991.

[2] Foster, J. E., Williams, G. J., and Patterson, M. J., "Characterization of an Ion Thruster Neutralizer," *J. Propul. Power*, Vol. 23, No. 4, 2007.

[3] Brophy, J. R., Garner, C. E., and Mikes, S. C., "Dawn Ion Propulsion System: Initial Checkout after Launch," *J. Propul. Power*, Vol. 25, No. 6, 2009, pp. 1189–1202.

[4] "NASA Earth Observatory," Online, 2000. URL `https://earthobservatory.nasa.gov/features/LearningToFly/fly_3.php`.

[5] Fearn, D. G., "Ion Thruster Thrust Vectoring Requirements and Techniques," *27th International Electric Propulsion Conference*, Pasadena, CA, 2001.

[6] Whealton, J., "Linear optics theory of ion beamlet steering," *Rev. Sci. Instrum.*, Vol. 48, No. 11, 1977, pp. 1428–1429.

[7] Homa, J., and Wilbur, P., "Ion beamlet vectoring by grid translation," *16th International Electric Propulsion Conference*, 1982, p. 1895.

[8] Stewart, L., Kim, J., and Matsuda, S., "Beam focusing by aperture displacement in multiampere ion sources," *Rev. Sci. Instrum.*, Vol. 46, No. 9, 1975, pp. 1193–1196.

[9] Adam, W., and Lathem, W., "Theoretical analysis of a grid-translation beam deflection system for a 30-cm diameter Kaufman thruster," *NASA Technical Memorandum*, , No. X-67911, 1971.

[10] Homa, J. M., "Ion Beamlet Steering for Two-Grid Electrostatic Thrusters," Master's thesis, Colorado State University, Fort Collins, CO, July 1984.

[11] Haag, T., "Translation Optics for 30 cm Ion Engine Thrust Vector Control," *27th International Electric Propulsion Conference*, Pasadena, CA, 2001.

[12] Okawa, Y., Hayakawa, Y., Miyazaki, K., and Kitamura, S., "Ion Thruster Thrust Vectoring by Grid Translation," *28th International Electric Propulsion Conference*, Toulouse, France, 2003.

[13] Shagayda, A., Nikitin, V., and Tomilin, D., "Three-dimensional analysis of ion optics with misalignments of apertures," *Vacuum*, Vol. 123, 2016, pp. 140–150.

[14] Brophy, J. R., Kakuda, R. Y., Polk, J. E., Anderson, J. R., Marcucci, M. G., Brinza, D., Henry, M. D., Fujii, K. K., Mantha, K. R., Stocky, J. F., Sovey, J., Patterson, M., Rawlin, V., Hamley, J., Bond, T., Christensen, J., Cardwell, H., Benson, G., Gallagher, J., Matranga, M., and Bushway, D., "Ion Propulsion System (NSTAR) DS1 Technology Validation Report," , 2000.

[15] Polk, J., Kakuda, J., Anderson, J., Brophy, J., Rawlin, V., Patterson, M., Sovey, J., and Hamley, J., "Performance of NSTAR Ion Propulsion System on the Deep Space One Mission," *39th Aerospace Sciences Meeting and Exhibit*, 2001, p. 965.

[16] Rayman, M. D., and Varghese, P., "The Deep Space 1 Extended Mission," *Acta Astronaut*, Vol. 48, No. 5-12, 2001, pp. 693–705.

[17] Rayman, M. D., "The Succesful Conclusion of the Deep Space 1 Mission: Important Results without a Flashy Title," *53rd International Astronautical Congress/World Space Congress*, 2002.

[18] "Dawn Mission Status," Online, 2018. URL `https://earthobservatory.nasa.gov/features/LearningToFly/fly_3.php`.

[19] Kaufman, H. R., "Technology of electron-bombardment ion thrusters," *Advances in Electronics and Electron Physics*, Vol. 36, Elsevier, 1975, pp. 265–373.

[20] Diaz, E. M., and Soulas, G. C., "Grid Gap Measurement for an NSTAR Ion Thruster," *29th International Electric Propulsion Conference*, Princeton, NJ, 2005.

[21] Wirz, R. E., Anderson, J. R., and Katz, I., "Time-dependent erosion of ion optics," *Journal of Propulsion and Power*, Vol. 27, No. 1, 2011, pp. 211–217.

[22] Soulas, G. C., "NEXT Thruster-Induced Roll Torque Due to Aperture Misalignment," NEXT Project Memorandum, 2009.

[23] Brophy, J. R., "Ion Thruster Produced Roll Torque," JPL Interoffice Memorandum, 2004. 353-04-017.

[24] Herman, D. A., Patterson, M. J., and Soulas, G. C., "NASA's Evolutionary Xenon Thruster (NEXT) Prototype-Model Ion Optics Operating Grid-Gap Measurements," *JANNAF Propulsion Meeting*, Orlando, FL, 2008.

[25] Yamashita, Y., Tsukizaki, R., Yamamoto, Y., Koda, D., Nishiyama, K., and Kuninaka, H., "Azimuthal Ion Drift of a Gridded Ion Thruster," *Plasma Sources Sci. Technol.*, Vol. 27, No. 105006, 2018.

[26] Yamashita, Y., Tsukizaki, R., Yamamota, Y., Koda, D., Nishiyama, K., and Kuninaka, H., "2DPIC Simulation and Laser-Induced Fluorescence Spectroscopy of the Roll Torque of the Gridded Ion Thruster," *54th Joint Propulsion Conference and Exhibit*, Cincinnati, OH, 2018.

[27] Tsukizaki, R., Yamamoto, Y., Koda, D., Yusuke, Y., Nishiyama, K., and Kuninaka, H., "Azimuthal Velocity Measurement in the Ion Beam of a Gridded Ion Thruster using Laser-Induced Fluorescence Spectroscopy," *Plasma Sources Sci. Technol.*, Vol. 27, No. 015013, 2018.

[28] Hudis, M., and Lidsky, L. M., "Directional Langmuir Probe," *J. Appl. Phys.*, Vol. 41, No. 12, 1970, pp. 5011–5017.

[29] Hutchinson, I. H., "Ion Collection by a Sphere in a Flowing Plasma," *Plasma Phys. Controlled Fusion*, Vol. 44, No. 9, 2002, pp. 1953–1977.

[30] Hutchinson, I. H., *Principles of Plasma Diagnostics*, 2nd ed., Cambridge University Press, Cambridge, MA, 2002. Electronic Book: `silas.psfc.mit.edu/introplasma/`.

[31] Oksuz, L., and Hershkowitz, N., "Understanding Mach Probes and Langmuir Probes in a Drifting, Unmagnetized, Non-Uniform Plasma," *Plasma Sources Sci. Technol.*, Vol. 13, No. 2, 2004, pp. 263–271.

[32] Thomas, R., "NEXT EM5 VF-16 Thrust Vector Data," Unpublished, 2019. NASA GRC Internal Memo.

[33] Farnell, C. C., Farnell, C. C., and Monheiser, J. M., "NEXT EM5 VF-6 Testing Thrust Vector Data," Unpublished, 2019. NEXT-C Project Data.

[34] Rayman, M. D., Fraschetti, T. C., Russell, C. T., and Raymond, C. A., "Dawn: A Mission In Development for Exploration of Main Belt Asteroids Vesta and Ceres," *Acta Astronautica*, Vol. 58, No. 11, 2006, pp. 605–616.

[35] Garner, C., and Rayman, M. D., "In-Flight Operation of the Dawn Ion Propulsion System Throuh Survey Science Orbit at Ceres," *51st AIAA/SAE/ASEE Joint Propulsion Conference*, Orlando, FL, 2015.

[36] Boeing and NASA Jet Propulsion Lab, "Dawn Flight Grids Assembled Alignment Data," Unpublished, 2007.

[37] Garner, C. E., Brophy, J. R., Mikes, S. C., and Rayman, M. D., "In-Flight Operation of the Dawn Ion Propulsion System–The First Nine Months," *44th AIAA/ASME/SAE/ASEE Joint Propulsion Conference*, Hartford, CT, 2008.

[38] Garner, C. G., and Rayman, M. D., "In-Flight Operation of the Dawn Ion Propulsion System Through Year Two of Cruise to Ceres," *50th AIAA/ASME/SAE/ASEE Joint Propulsion Conference*, Cleveland, OH, 2014.

[39] Soulas, G. C., and Shastry, R., "Post-Test Inspection of NASA's Evolutionary Xenon Thruster Long Duration Test Hardware: Ion Optics," *52nd AIAA/SAE/ASEE Joint Propulsion Conference*, Salt Lake City, UT, 2016.

[40] Soulas, G. C., Kamhawi, H., Patterson, M. J., Britton, M. A., and Frandina, M. M., "NEXT ion Engine 2000 Hour Wear Test Results," *40th AIAA/ASME/SAE/ASEE Joint Propulsion Conference and Exhibit*, Fort Lauderdale, FL, 2004.